Bettina Rendenbach, Steffen Klenner, Rainer Pöttgen and Dirk Johrendt*

Magnetic and electronic properties of $CaFeO_2Cl$

https://doi.org/10.1515/znb-2019-0160
Received October 10, 2019; accepted October 24, 2019

Abstract: $CaFeO_2Cl$ is a unique exception in the family of the iron oxyhalides. Its crystal structure is not related to the Ruddlesden-Popper phases as known for the other members, but contains layers of edge-sharing $FeO_{2/2}O_{3/3}$ pyramids without Fe–Cl contacts. The iron atoms form a distorted honeycomb substructure. Magnetization measurements on single crystals show an unexpected weak anisotropy and indicate antiferromagnetic ordering of the iron magnetic moments already at room temperature. ^{57}Fe Mössbauer spectra confirm the trivalent oxidation state of iron and the presence of magnetic order. DFT calculations using the LDA + U approach support a Mott-insulating antiferromagnetic ground state and indicate a Néel-type ordered antiferromagnetic state in the honeycomb layer. The band gap from optical measurements is 1.3 eV and agrees with the red-brown colour as well as with the theoretical calculations.

Keywords: DFT calculations; honeycomb lattice; iron oxyhalide; magnetism; Mott-insulator.

Dedicated to: Professor Arndt Simon on the occasion of his 80th birthday.

1 Introduction

The search for new layered materials produced various mixed anion compounds [1, 2], such as oxide carbonates [3], oxide borates [4] and oxide halides [5, 6]. Especially layered oxyhalides represent a promising field for studies of new materials with various properties [7], such as superconductors [8], frustrated magnets [9], or possible two-dimensional magnetism challenging the Mermin-Wagner theorem [10]. The research also led to an awaking interest in oxyhalides as high-T_c multiferroics [11], and especially in high-T_c materials, resulting in several copper oxide halide superconductors [12–15].

Iron oxyhalides with alkaline earth cations have been reported with different structure types, among them AE_2FeO_3X (AE = Ca, Sr, X = F, Cl, Br) and $Sr_3Fe_2O_5Cl_2$. These derivatives of the tetragonal K_2NiF_4-type or Ruddlesden-Popper phases [16, 17] contain layers or double layers of $Fe(O, X)_6$ octahedra with the halides X at the apical positions. Neutron scattering experiments revealed antiferromagnetic ordering with magnetic moments orientated parallel to the layers, e.g. G-type antiferromagnetism in $Sr_3Fe_2O_5Cl_2$ [18]. Belonging to this class of layered transition metal halides, monoclinic $CaFeO_2Cl$ [19, 20] is exceptional because the structure contains no octahedra but consists of layers of edge-sharing $FeO_{2/2}O_{3/3}$ square pyramids separated by CaCl sheets; no Fe–Cl contacts occur (Fig. 1). The iron atoms form a distorted honeycomb substructure on the *ab* plane.

In spite of the exceptional crystal structure, the physical properties of $CaFeO_2Cl$ are currently unknown. We have optimized the synthesis procedure given in the literature [19] and achieved samples with purities above 90%. In this paper, we report results of magnetic and optical measurements, along with quantum chemical calculations. We show that $CaFeO_2Cl$ is an antiferromagnetic Mott insulator and propose a probable magnetic ordering pattern.

2 Experimental

2.1 Synthesis

$CaFeO_2Cl$ was synthesized by a modified procedure of the protocol reported by J. Ackermann [19]. The starting materials Fe_2O_3 (Alfa Aesar, 99.99%), and $CaCl_2$ (ABCR, 99.99%), were mixed in a ratio 1:100 and ground in an agate mortar in air. The samples were prepared in alumina crucibles under air by heating to 850°C for 12 h, then cooled to 350°C for 5 h, and finally cooled to room temperature (step 1). After grounding the samples obtained in step one, the procedure from step one was repeated with a slower cooling rate of 20 K h^{-1} (step 2). Washing the product several times with distilled water removed all excess $CaCl_2$. The resulting samples were dried under vacuum and stored under argon. This approach yielded a polycrystalline red-brown powder with brown plate-like single crystals. The samples

***Corresponding author: Dirk Johrendt,** Department Chemie, Ludwig-Maximilians-Universität München, Butenandtstraße 5–13 (Haus D), 81377 München, Germany, e-mail: johrendt@lmu.de
Bettina Rendenbach: Department Chemie, Ludwig-Maximilians-Universität München, Butenandtstraße 5–13 (Haus D), 81377 München, Germany
Steffen Klenner and Rainer Pöttgen: Institut für Anorganische und Analytische Chemie, Universität Münster, Corrensstraße 30, 48149 Münster, Germany

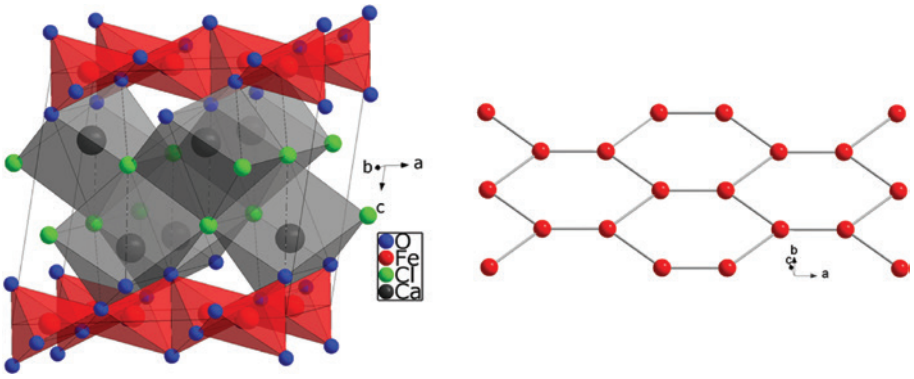

Fig. 1: Crystal structure of monoclinic $CaFeO_2Cl$. Left: Unit cell with the layers of $FeO_{2/2}O_{3/3}$ square pyramids (red polyhedra) emphasized. Right: Distorted honeycomb substructure of the Fe atoms.

contained the desired product $CaFeO_2Cl$ and some unreacted Fe_2O_3. Through this optimized synthesis, yields of up to 92% were achieved.

2.2 X-ray diffraction and structure refinement

The powder X-ray patterns were obtained with a STOE Stadi-P diffractometer (Mo$K\alpha_1$ radiation) equipped with a STOE Mythen 1k detector. Rietveld refinement were done with Topas [21]. Single-crystal diffraction data was recorded with a STOE IPDS-I diffractometer at room temperature using Mo$K\alpha_1$ radiation ($\lambda = 0.71069$ Å). Reflection intensity integration, data reductions, and multi-scan absorption corrections were performed with Apex2 [22] and Sadabs [23]. The structure was solved with Jana2006 [24] and refined with the Shelxl crystallographic software package [25].

CCDC 1957141 contains the supplementary crystallographic data for this paper. These data can be obtained free of charge from The Cambridge Crystallographic Data Centre via www.ccdc.cam.ac.uk/data_request/cif.

2.3 Magnetic measurements

Magnetic measurements with $CaFeO_2Cl$ single crystals were carried out with a vibrating sample magnetometer (VSM) option in a Quantum Design Physical-Property-Measurement-System (PPMS-9). Crystals were selected manually from the samples, aligned parallel to the *ab* crystal plane of $CaFeO_2Cl$ in a parquet-like pattern and glued with low temperature varnish. Magnetization measurements were carried out with the *ab* crystal plane parallel and perpendicular to the magnetic field.

2.4 Electronic structure DFT calculations

Electronic structure calculations were performed using the Vienna ab initio simulation package (Vasp) [26, 27] which is based on density functional theory (DFT) and plane wave basis sets. Projector-augmented waves (PAW) [28] were used and contributions of correlation and exchange were treated in the generalized-gradient approximation (GGA) [29]. The strongly correlated Fe 3*d* states were corrected using the LDA + *U* method in the rotationally invariant approach by Dudarev et al. [30].

2.5 Optical measurements

Diffuse reflectance spectra were measured with powder samples on a UV/Vis Jasco V-650 spectrophotometer (200–800 nm). The spectra were converted to absorption spectra based on the Kubelka-Munk [31] theory to determine the optical band gap.

2.6 Mössbauer spectroscopic measurements

A ^{57}Co source in a Rh matrix was used for the ^{57}Fe Mössbauer spectroscopic investigation of $CaFeO_2Cl$. The measurement was performed in a continuous-flow cryostat system (Janis Research Co LLC). The usual transmission geometry was used. The source was kept at room temperature while the sample was cooled to $T = 6$ K. The optimal absorber thickness was calculated according to the work of Long et al. [32]. The sample was placed in a thin-walled PMMA container and diluted with potassium chloride for a complete distribution of the sample within the container volume. Fitting of the experimental data was performed with the WinNormos for Igor6 program package [33].

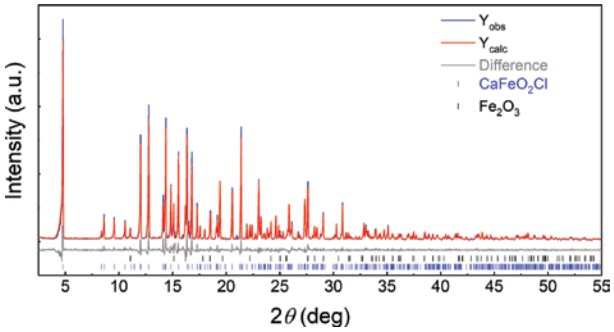

Fig. 2: X-ray powder pattern (Mo$K\alpha_1$) of the $CaFeO_2Cl$ sample (blue) with Rietveld fit (red) and difference line (grey line).

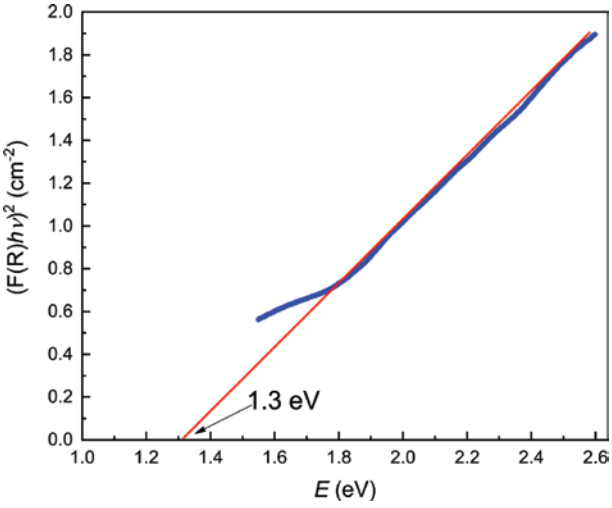

Fig. 3: Band gap calculation using the Kubelka-Munk function.

3 Results

3.1 Synthesis and crystal structure

$CaFeO_2Cl$ was synthesized in a $CaCl_2$ flux in an open system from Fe_2O_3 as a red-brown, moisture and air stable product. Single-crystal X-ray diffraction data confirmed the structure in the monoclinic centrosymmetric space group $C2/m$ (No. 12) with the lattice parameters $a = 9.969(2)$, $b = 3.811(8)$, $c = 8.735(17)$ Å and $\beta = 103.62(3)°$. The single-crystal X-ray data was used to refine the powder X-ray pattern (Fig. 2). The Rietveld fit yielded $CaFeO_2Cl$ as the main component (ca. 92 wt.%) with Fe_2O_3 as impurity.

Figure 1 shows the crystal structure of $CaFeO_2Cl$. Layers of edge sharing $FeO_{2/2}O_{3/3}$ polyhedra alternate with regions of CaCl. The FeO_5 pyramid is slightly distorted with four different Fe–O distances ranging from 1.89 to 2.00 Å. The Addison τ parameter ($\tau = (\beta - \alpha)/60$; α, β = largest bond angles) [34] of 0.1 confirms the square pyramidal coordination. Calcium has three oxygen and four chlorine neighbours. The iron substructure is a planar but slightly elongated honeycomb net with Fe–Fe distances of 2.743 and 2.959 Å.

3.2 Optical properties

Figure 3 shows the results of an optical reflection measurement of the $CaFeO_2Cl$ powder ($\lambda = 500$–800 nm). Because weak signals in absorbance spectra are enhanced in reflected spectra, reflectance spectra in absorbance units cannot be compared directly. Analyzing reflection spectra using the Kubelka-Munk function makes them similar to absorbance spectra and allows the determination of the band gap energy E_g [31].

$$F(R_\infty) = \frac{1 - R_\infty}{R_\infty} = \frac{K(\lambda)}{s(\lambda)} \propto \alpha = \frac{(h\nu - E_g)^2}{h\nu}$$

R_∞ is the diffuse reflectance of an infinitely thick sample, $K(\lambda)$ is the absorption coefficient and $s(\lambda)$ is the scattering coefficient. The band gap is determined by the extrapolation from the linear portion of the plot of $[F(R_\infty)h\nu]^2$ against $h\nu$ (Tauc plot). The estimated band gap is 1.3 eV (Fig. 3), which is consistent with the red-brown color of $CaFeO_2Cl$.

3.3 Magnetism

Selected plate-like single crystals of $CaFeO_2Cl$ were arranged parallel on the sample holder in order to measure the magnetization in fields applied either perpendicular ($\perp$) or parallel (//) to the layers. Note that the crystals were not aligned along the directions perpendicular to the layers. Figure 4 shows magnetization isotherms at temperatures between 5 and 305 K.

The magnetization increases linearly with the field strength but remains below 0.05 μ_B per formula unit $CaFeO_2Cl$, which indicates that the magnetic moments of the Fe^{3+} ions ($S = 5/2$) are antiferromagnetically ordered in the considered temperature range (5–300 K). The magnetization increases at lower temperatures, which is contrary to the expected either constant values if the field is perpendicular or a decrease if it is parallel to the magnetization direction (easy axis) of an antiferromagnet [35]. Given that the magnetization remains very small even at low temperatures, the increase may

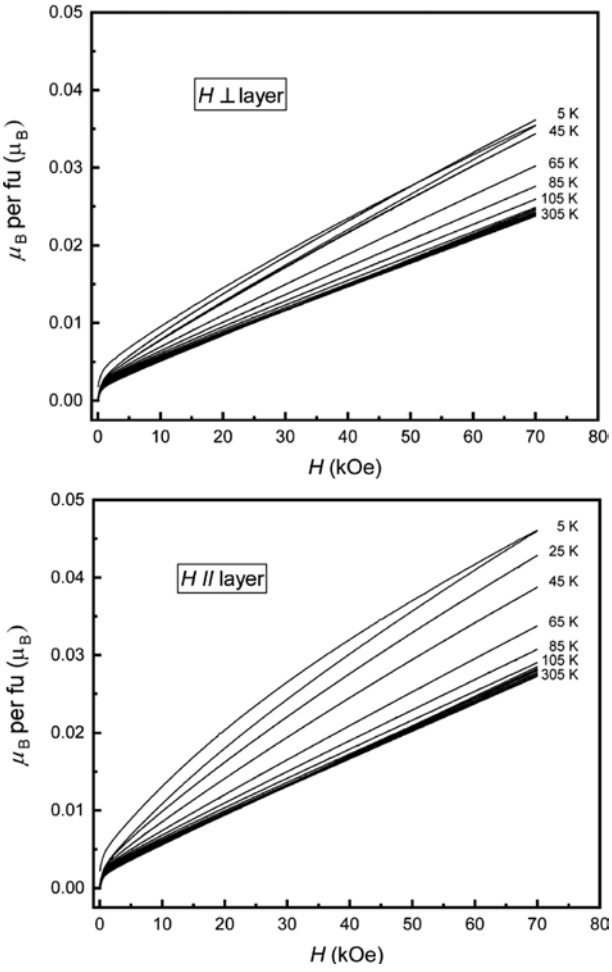

Fig. 4: Magnetization isotherms of $CaFeO_2Cl$ between $T = 5$ and 305 K with fields aligned perpendicular (top) and parallel to the FeO_2 layers (bottom). (fu = formula unit; 1 kOe = 7.96×10^4 A m^{-1})

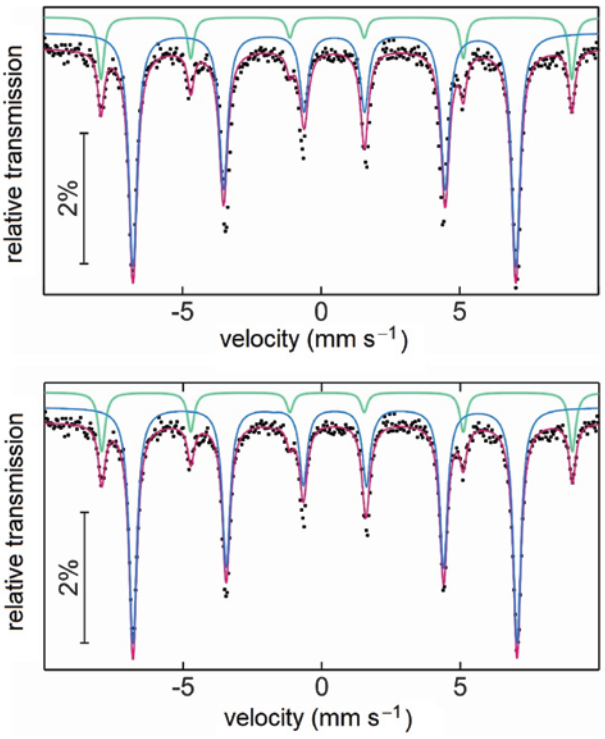

Fig. 5: Experimental (black dots) and simulated (colored lines) ^{57}Fe Mössbauer spectra of $CaFeO_2Cl$ at $T = 6$ K. Top: $CaFeO_2Cl$ signal fitted with a sextet model; bottom: $CaFeO_2Cl$ fitted with a complete Hamiltonian.

be the result of traces of paramagnetic impurities. The anisotropy of the magnetization is relatively small with respect to the layered crystal structure. Assuming that the paramagnetic contributions (from impurities) are isotropic, we find that the magnetization at $T = 5$ K is about 25% higher if the field is parallel to the $FeO_{2/2}O_{3/3}$ layers. This indicates that the alignment of the magnetic moments, or easy axis, should be perpendicular to the layers.

3.4 Mössbauer spectroscopy

The ^{57}Fe spectrum of polycrystalline $CaFeO_2Cl$ at $T = 6$ K is shown in Fig. 5. The corresponding fitting parameters for the most reliable fit are listed in Table 1. Figure 5 shows two different fitting approaches. Two overlapping sextet signals are visible in the recorded spectrum. The less intense one corresponds to the by-product Fe_2O_3 and the other one to $CaFeO_2Cl$. The top spectrum of Fig. 5 shows a fit with two regular sextets, the bottom one a fitting with a full Hamiltonian. No impurity phases other than Fe_2O_3 can be observed in the experimental spectrum, in accordance with the PXRD data. It is clearly apparent that the fit for the top spectrum is slightly off-centered from the normal sextet splitting. The full Hamiltonian fit with the inclusion of the parameter θ, which describes the angle between the direction of the magnetic hyperfine field and the tensor of the electrical field gradient, gives a more satisfactory fitting. Similar results have recently been reported for the brownmillerite phase $Sr_2Fe_2O_5$ [36].

The isomer shift of 0.30 mm s^{-1} indicates iron in the oxidation state +3 as can be expected from the empirical formula. This is in agreement with a large collection of ^{57}Fe data of iron oxides compiled by Menil [37]. The square pyramidal coordination of Fe(III) is rare; however, our ^{57}Fe Mössbauer spectroscopic data is in good agreement with the series of iron substituted chromates $RETiCr_{1-x}Fe_xO_5$ [38].

The slightly negative quadrupole splitting of −0.97 mm s^{-1} results from the asymmetric coordination environment

Table 1: Fitting parameters of the 6 K ^{57}Fe Mössbauer spectroscopic measurements of $CaFeO_2Cl$.

	δ (mm s^{-1})	ΔE_Q (mm s^{-1})	Γ (mm s^{-1})	B_{hf} (T)	θ (deg)	Area (%)
$CaFeO_2Cl$	0.30(1)	−0.97(1)	0.337(3)	42.6(1)	39.9(2)	82(1)
Fe_2O_3	0.37(1)	0.37(1)	0.287(12)	52.6(1)	–	18(1)

δ, isomer shift; ΔE_Q, quadrupole splitting; Γ, experimental line width; B_{hf}, magnetic hyperfine field; θ, tensor between the principle axis of the electrical field gradient and the direction of the magnetic hyperfine field.

of the iron site (distorted square pyramid). Full magnetic hyperfine field splitting is observed with a field of 42.6 T. The parameter θ mentioned above leads to the conclusion that the magnetic moments are aligned along a preferred crystallographic direction.

3.5 DFT calculations

The electronic band structure was calculated using the VASP package. Due to the actually unknown magnetic structure, the total energies of different trial magnetic ordering patterns were compared in order to identify a probable magnetic state. The primitive unit cell of $CaFeO_2Cl$ contains four iron positions. The trial magnetic structures were either ferromagnetic (FM ↑↑↑↑), or antiferromagnetic (AF1 ↑↓↑↓; AF2 ↑↓↓↑; AF3 ↑↑↓↓). The calculations have revealed that AF1 is the most stable configuration, followed by AF2 (+0.1 eV), AF3 (+0.36 eV) and FM (+0.4 eV). AF1 corresponds to a Néel-type magnetic structure where all moments of the iron atoms within the honeycomb layer are alternating spin up and down as shown in Fig. 6.

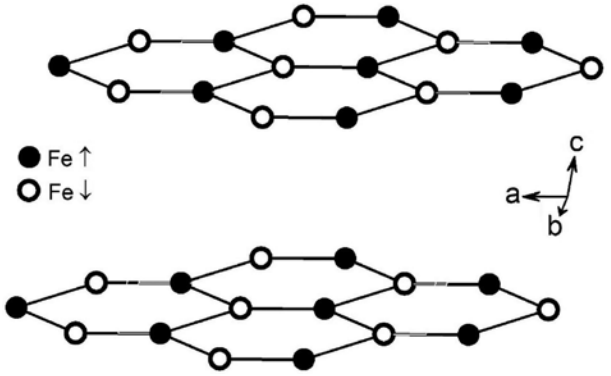

Fig. 6: Most stable trial AF magnetic structure in the honeycomb Fe layer of $CaFeO_2Cl$. Filled and open circles mark spin up and down, respectively.

The spin-polarized band structure shown in Fig. 7 was calculated using this model of the antiferromagnetic ordering and the LDA + U approach with a U_{eff} (= U–J; J = 0) of 4 eV in order to account for the strongly correlated Fe-3d states. The calculated band gap E_g occurs between the O-2p valence bands and Fe-3d conduction bands. E_g correlates linearly with the U_{eff} parameter and results in 1.96 eV for U = 4 eV and 1.59 eV for U = 3 eV. The calculated ordered magnetic moment of 4.2–4.3 μ_B per Fe atom is smaller than the expected 5 μ_B per Fe atom for the S = 5/2 state. This may have its origin in the special magnetic properties of the honeycomb substructure with only three neighbors. It has been shown that the magnetization in a threefold connected S = 1/2 system is reduced by a factor of 0.87 compared to the square lattice [39]. A reduced ordered magnetic moment of 2.3 μ_B has also

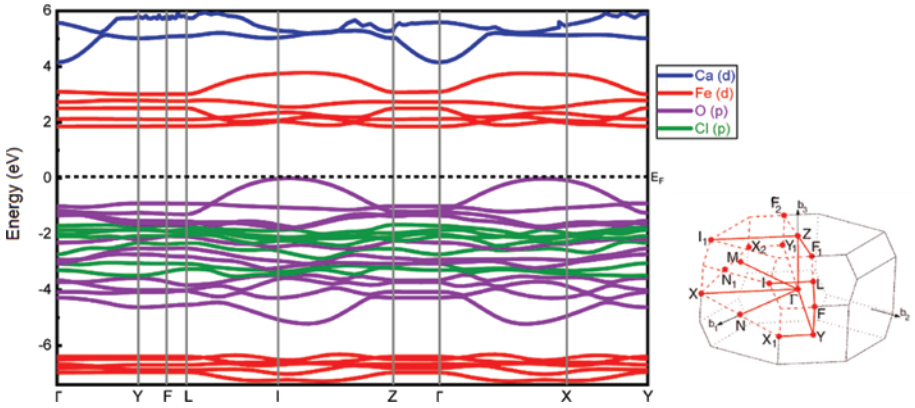

Fig. 7: Spin polarized LDA + U band structure of antiferromagnetic $CaFeO_2Cl$.

been found in the $S = 3/2$ antiferromagnetic honeycomb lattice of Li_2MnO_3 [40].

4 Conclusion

$CaFeO_2Cl$ was obtained in an open system synthesis from Fe_2O_3 in a $CaCl_2$ flux. The single-crystal and powder X-ray data confirm the layered crystal structure with five-fold coordinated iron as described earlier. Magnetic measurements with orientated single crystals indicate that the magnetic moments at the iron atoms are antiferromagnetically ordered at room temperature and suggest that the magnetic easy axis is perpendicular to the layers. ^{57}Fe Mössbauer spectra confirm the trivalent oxidation state of iron and the magnetic ordering showing full magnetic hyperfine splitting with a field of 42.6 T at 6 K. $CaFeO_2Cl$ is a Mott insulator with an optical band gap of ~1.3 eV. DFT electronic band structure calculations using the LDA + U approach confirm the measured properties and suggest that the magnetic ordering pattern is of Néel-type within a honeycomb-like layer of iron atoms.

References

[1] M. T. Weller, C. S. Knee, *J. Mater. Chem.* **2001**, *11*, 701–712.
[2] G. M. Veith, M. Greenblatt, M. Croft, J. B. Goodenough, *Mater. Res. Bull.* **2001**, *36*, 1521–1530.
[3] K. Yamaura, Q. Huang, J. W. Lynn, R. W. Erwin, R. J. Cava, *J. Solid State Chem.* **2000**, *152*, 374–380.
[4] D. Pelloquin, M. Hervieu, C. Michel, N. Nguyen, B. Raveau, *J. Solid State Chem.* **1997**, *134*, 395–408.
[5] W. Leib, Hk. Müller-Buschbaum, *Z. Anorg. Allg. Chem.* **1984**, *518*, 115–119.
[6] J. Huang, R.-D. Hoffmann, A. W. Sleight, *Mater. Res. Bull.* **1990**, *25*, 1085–1090.
[7] M. Ai-Mamouri, P. P. Edwards, C. Greaves, M. Slaski, *Nature* **1994**, *369*, 382.
[8] S. Adachi, T. Tatsuki, T. Tamura, K. Tanabe, *Chem. Mater.* **1998**, *10*, 2860–2869.
[9] A. A. Tsirlin, H. Rosner, *Phys. Rev. B: Condens. Matter.* **2009**, *79*, 214416.
[10] N. D. Mermin, H. Wagner, *Phys. Rev. Lett.* **1966**, *17*, 1133–1136.
[11] L. Zhao, M. T. Fernández-Díaz, L. H. Tjeng, A. C. Komarek, *Sci. Adv.* **2016**, *2*, e1600353.
[12] S. M. Loureiro, C. Felser, Q. Huang, R. J. Cava, *Chem. Mater.* **2000**, *12*, 3181–3185.
[13] N. D. Zhigadlo, J. Karpinski, S. Weyeneth, R. Khasanov, S. Katrych, P. Wägli, H. Keller, *J. Phys. Conf. Ser.* **2008**, *97*, 012121.
[14] X. J. Wu, C. Q. Jin, P. Laffez, T. Tatsuki, T. Tamura, S. Adachi, H. Yamauchi, N. Koshizuka, *Physica C* **1996**, *258*, 143–152.
[15] Q. Q. Liu, X. M. Qin, Y. Yu, F. Y. Li, C. Dong, C. Q. Jin, *Physica C* **2005**, *420*, 23–29.
[16] S. N. Ruddlesden, P. Popper, *Acta Crystallogr.* **1957**, *10*, 538–539.
[17] S. N. Ruddlesden, P. Popper, *Acta Crystallogr.* **1958**, *11*, 54–55.
[18] C. S. Knee, M. A. L. Field, M. T. Weller, *Solid State Sci.* **2004**, *6*, 443–450.
[19] J. F. Ackerman, *J. Solid State Chem.* **1991**, *92*, 496–513.
[20] E. Parthé, S. Hu, *J. Solid State Chem.* **2003**, *174*, 165–166.
[21] A. Coelho, Topas-Academic (version 4.1), Coelho Software, Brisbane (Australia) **2007**.
[22] Apex2, Bruker AXS Inc., Madison, WI (USA) **2007**.
[23] G. M. Sheldrick, Sadabs (version 2012/1), Bruker AXS Inc., Madison, WI (USA) **2001**.
[24] V. Petříček, M. Dušek, L. Palatinus, Jana2006, The Crystallographic Computing System, Institute of Physics, Academy of Sciences of the Czech Republic, Prague (Czech Republic) **2006**.
[25] G. Sheldrick, *Acta Crystallogr.* **2008**, *A64*, 112–122.
[26] G. Kresse, J. Furthmüller, *Comput. Mat. Sci.* **1996**, *6*, 15–50.
[27] G. Kresse, D. Joubert, *Phys. Rev. B* **1999**, *59*, 1758–1775.
[28] P. E. Blöchl, *Phys. Rev. B* **1994**, *50*, 17953–17979.
[29] J. P. Perdew, K. Burke, M. Ernzerhof, *Phys. Rev. Lett.* **1996**, *77*, 3865–3868.
[30] S. L. Dudarev, G. A. Botton, S. Y. Savrasov, C. J. Humphreys, A. P. Sutton, *Phys. Rev. B* **1998**, *57*, 1505–1509.
[31] P. Kubelka, F. Munk, *Z. Tech. Phys.* **1931**, *12*, 593.
[32] G. J. Long, T. E. Cranshaw, G. Longworth, *Moessbauer Eff. Ref. Data J.* **1983**, *6*, 42.
[33] R. A. Brand, WinNormos for Igor6 (version for Igor 6.2 or above: 22/02/2017), Universität Duisburg, Duisburg (Germany) **2017**.
[34] A. W. Addison, T. N. Rao, J. Reedijk, J. van Rijn, G. C. Verschoor, *J. Chem. Soc., Dalton Trans.* **1984**, 1349–1356.
[35] T. Nagamiya, K. Yosida, R. Kubo, *Adv. Phys.* **1955**, *4*, 1–112.
[36] J. C. Waerenborgh, E. V. Tsipis, J. E. Auckett, C. D. Ling, V. V. Kharton, *J. Solid State Chem.* **2013**, *205*, 5–9.
[37] F. Menil, *J. Phys. Chem. Solids.* **1985**, *46*, 763–789.
[38] P. J. Schurer, A. H. Morrish, *Phys. Rev. B* **1977**, *16*, 951–959.
[39] R. F. Bishop, P. H. Y. Li, O. Götze, J. Richter, C. E. Campbell, *Phys. Rev. B* **2015**, *92*, 224434.
[40] S. Lee, S. Choi, J. Kim, H. Sim, C. Won, S. Lee, S. A. Kim, N. Hur, J.-G. Park, *J. Phys.: Condens. Matter* **2012**, *24*, 456004.